

# Transfer of CD11c<sup>+</sup> lamina propria mononuclear phagocytes from post-infectious irritable bowel syndrome causes mucosal barrier dysfunction and visceral hypersensitivity in recipient mice

YA-JUN REN<sup>1</sup>, LEI ZHANG<sup>2</sup>, TAO BAI<sup>2</sup>, HONG-LU YU<sup>1</sup>, YING LI<sup>2</sup>, WEI QIAN<sup>2</sup>,  
SI JIN<sup>3</sup>, ZHI-FAN XIONG<sup>1</sup>, HUAN WANG<sup>2</sup> and XIAO-HUA HOU<sup>2</sup>

<sup>1</sup>Division of Gastroenterology, Liyuan Hospital, Tongji Medical College, Huazhong University of Science and Technology, Wuhan, Hubei 430077; <sup>2</sup>Division of Gastroenterology, Union Hospital, Tongji Medical College, Huazhong University of Science and Technology, Wuhan, Hubei 430022; <sup>3</sup>Department of Endocrinology, Institute of Geriatric Medicine, Liyuan Hospital, Tongji Medical College, Huazhong University of Science and Technology, Wuhan, Hubei 430077, P.R. China

Received August 8, 2016; Accepted April 12, 2017

DOI: 10.3892/ijmm.2017.2966

**Abstract.** The role of low-grade inflammation in the development of post-infectious irritable bowel syndrome (PI-IBS) has attracted increasing attention. Abnormal CD11c<sup>+</sup> mononuclear phagocytes, such as dendritic cells (DCs), macrophages, and monocytes, are involved in the disruption of immune tolerance in organisms, which can lead to the development of chronic inflammatory diseases. The present study tested the hypothesis that CD11c<sup>+</sup> lamina propria mononuclear phagocytes (CD11c<sup>+</sup> LPMPs) contribute to increased mucosal permeability and visceral hypersensitivity in a PI-IBS mouse model. CD11c<sup>+</sup> LPMPs were isolated and purified via the digestion of intestinal tissues and magnetic-activated cell sorting. We detected increased mucosal permeability, visceral hypersensitivity and intestinal inflammation during both the acute and chronic stages of *Trichinella* infection. Following the transfer of CD11c<sup>+</sup> LPMPs from PI-IBS mice into normal mice, low-grade inflammation was detected, as demonstrated by increased IL-4 expression in the ileum, as well as enhanced mucosal permeability, as indicated by decreased transepithelial electrical resistance and the presence of ultrastructural

alterations. More importantly, the mice that underwent adoptive transfer of CD11c<sup>+</sup> LPMPs from the PI-IBS mice also exhibited increased abdominal withdrawal reflex scores and a decreased threshold. Our data demonstrated that the CD11c<sup>+</sup> LPMPs from this PI-IBS mouse model were not only able to transfer enteric inflammation to the normal mice but also caused abnormal intestinal function, characterized by epithelial barrier disruption and visceral hyperalgesia.

## Introduction

Dysfunction and destruction of the intestinal epithelial barrier results in an increased mucosal antigen load, leading to the activation of mucosal immune responses (1,2), which are associated with the pathogenesis of several intestinal disorders, including irritable bowel syndrome (IBS) (3-5). Barrier dysfunction has been documented in many patients with IBS, and it is especially common in those with post-infectious irritable bowel syndrome (PI-IBS) (6-8). Notably, increasing evidence indicates that PI-IBS may result from a combined process involving barrier dysfunction, low-grade mucosal inflammation and immune activation (5,9,10).

Intestinal inflammation has attracted increasing concern in relation to the pathogenesis of PI-IBS. Increased numbers of immune cells, primarily T cells and mast cells, have been detected in the colons (11), ilea and duodena (12-14) of subsets of IBS patients. Additionally, PI-IBS patients have significantly increased proportions of CD45RO<sup>+</sup>CD4<sup>+</sup> activated/memory T cells in the lamina propria (15). Interestingly, the number of T cells that infiltrate into the lamina propria is associated with the severity of diarrhea (16,17). Some studies have also demonstrated that the levels of inflammatory cytokines, including IL-1 $\beta$  and IFN- $\gamma$ , are increased in the intestines (18,19). Therefore, the proliferation and activation of T lymphocytes play important roles in the development and progression of IBS. Intestinal inflammation and immune system activation, particularly T lymphocyte activation, may contribute to the sensitization of peripheral or spinal nociceptive pathways and cause pain and

---

*Correspondence to:* Professor Zhi-Fan Xiong, Division of Gastroenterology, Liyuan Hospital, Tongji Medical College, Huazhong University of Science and Technology, 39 Yanhu Street, Wuhan, Hubei 430077, P.R. China  
E-mail: xiongzhi@126.com

Dr Huan Wang, Division of Gastroenterology, Union Hospital, Tongji Medical College, Huazhong University of Science and Technology, 1277 Jiefang Avenue, Wuhan, Hubei 430022, P.R. China  
E-mail: wanghuan508524@163.com

**Key words:** CD11c<sup>+</sup> lamina propria mononuclear phagocytes, mucosal barrier dysfunction, visceral hypersensitivity, mild inflammation, post-infectious irritable bowel syndrome model

hypersensitivity in PI-IBS patients (20). However, the reason why intestinal T lymphocytes are activated after gastrointestinal infection remains unclear. As the primary barrier, the intestine is exposed to a wide variety of antigens and bacteria, and it plays an important role in maintaining homeostasis in the body. Abnormal CD11c<sup>+</sup> mononuclear phagocytes, such as dendritic cells (DCs), macrophages, and monocytes, are involved in the disruption of immune tolerance in organisms, which can lead to the development of chronic inflammatory diseases, including Crohn's disease and others (21,22). Notably, different subtypes of mononuclear phagocytic cells play different roles. CD11c<sup>+</sup> monocytes/macrophages promote *Helicobacter hepaticus*-induced intestinal inflammation through the production of IL-23 (23). In addition, in *Citrobacter rodentium* infection, colonic CX3CR1<sup>+</sup> mononuclear phagocytes have been shown to induce an innate immune response (24). Furthermore, phenotypic and functional alterations in lamina propria dendritic cells (LPDCs) have been suggested to be at least partly responsible for activation of the effector pathways that lead to inflammatory bowel disease (25-28). In a previous study, we documented functional and phenotypic alterations of CD11c<sup>+</sup> lamina propria mononuclear phagocytes (CD11c<sup>+</sup> LPMPs) in a PI-IBS mouse model (29). These CD11c<sup>+</sup> LPMPs were more mature, expressed a greater number of co-stimulatory molecules, such as CD86 and MHCII, compared with that in control mice, and they induced T cell differentiation and cytokine expression. Another study reported that the number of CD103<sup>+</sup> LPDCs was found to be increased and that IL-4 was secreted to activate mast cells in an IBS rat model (30). However, the relationship between changes in CD11c<sup>+</sup> LPMPs and visceral hypersensitivity in the PI-IBS model remains unknown. Additionally, immune system activation and increased intestinal permeability often interact and promote each other. Thus, it is worthwhile to investigate whether CD11c<sup>+</sup> LPMPs promote dysfunction of the mucosal barrier in a PI-IBS model.

Currently, there is little evidence regarding the role of CD11c<sup>+</sup> LPMPs in IBS. The *Trichinella spiralis* (*T. spiralis*) infection mouse model used in our previous study is an effective model for elucidating the contribution of these cells to PI-IBS (29). Given the critical functions of CD11c<sup>+</sup> LPMPs in the intestinal immune system and their putative relationship with mucosal immune activation, we adoptively transferred these cells from PI-IBS model mice into naïve mice to test our hypothesis that they contribute to increased intestinal permeability and visceral hypersensitivity in PI-IBS.

## Materials and methods

**Mice and *Trichinella* infection.** Male NIH Swiss mice aged 6-8 weeks were obtained from the Guangdong Medical Laboratory Animal Center (Guangdong, China). The mice were housed under specific pathogen-free conditions at the Animal Laboratory Center of Tongji Medical College (Wuhan, China). They were housed individually at a temperature of 23-24°C with a light-dark cycle of 12-12 h and were allowed free access to standard mouse food and water. Each mouse was gavaged with 350-400 *T. spiralis* larvae in 0.2 ml phosphate-buffered saline (PBS). *T. spiralis* cultures were acquired from the Department of Parasitology and Microbiology, Tongji Medical College (Wuhan, China). All experiments were approved by

the Ethics Committee of Tongji Medical College, Huazhong University of Science and Technology.

**Abdominal withdrawal reflex (AWR) in response to colorectal distension (CRD).** The CRD protocol was performed as previously described (31). Briefly, a catheter with a balloon was coated with lubricant and inserted 2 cm from the anal verge. The behavioral response to CRD was assessed based on the AWR using a semi-quantitative scoring system (32). AWR scores were recorded following the application of ascending-limit phasic distension (20, 40, 60 and 80 mmHg) for 20 sec every 4 min. Measurement of the AWR score was repeated three times at each pressure value. The CRD stimulus intensity that elicited contraction of the abdominal wall was recorded as the threshold. Each balloon inflation value was recorded five times by an observer in a blinded manner to ensure for accuracy. More than six mice were included in each group.

**Pathological characteristics.** The mice were sacrificed by cervical dislocation, and ileal samples were fixed in buffered 10% formalin. Paraffin-embedded tissues were cut into 5 µm sections and stained with hematoxylin and eosin (H&E).

**Permeability assessment.** The ileum was quickly removed from each mouse and flushed with ice-cold Krebs solution (121 mM NaCl, 25 mM NaHCO<sub>3</sub>, 3.8 mM KCl, 1 mM KH<sub>2</sub>PO<sub>4</sub>, 1.2 mM CaCl<sub>2</sub>, 1.2 mM MgSO<sub>4</sub> and 11.1 mM glucose). The external muscle tissue and myenteric plexus were stripped off of the intestinal specimen. Sections of ileal villus epithelium were macroscopically identified as previously described (33,34). Each piece was placed in a Ussing chamber (Physiology Instruments, Santiago, CA, USA), and both sides of the chamber were filled with 5 ml Krebs solution, which was oxygenated, and maintained at 37°C throughout the experiment. The spontaneous potential difference and short circuit current in the Ussing chambers were recorded after a 25 min equilibration period. Transepithelial electrical resistance was calculated with Acquire and Analyze 2.3 software.

Three milliliters of FITC-dextran (FD4, 1 mg/ml; Sigma-Aldrich, St. Louis, MO, USA) were added to the mucosal side of each chamber, and an equivalent volume of Krebs solution was added to the other side. At 30-min intervals, 100 µl samples were collected and transferred to 96-well plates in duplicate. Krebs solution (200 µl) was added to the Ussing chambers after fluid collection to equalize the volumes. FD4 flux in each sample was measured at 520 nm with a fluorescence microplate reader (Molecular Devices, LLC, Sunnyvale, CA, USA). The FD4 concentration was determined based on standard curves as previously described (35). The permeability of each piece of tissue was presented as the calculated FD4 flux over a 60-90 min period. More than six mice were included in each group.

**Transmission electron microscopy.** Tissues were processed for transmission electron microscopic observations using modified standard procedures (36). The tissues were fixed in 2.5% buffered glutaraldehyde for 2 h at 4°C and were subsequently fixed in 1% osmium tetroxide for 2 h at room temperature. Then, they were dehydrated in graded alcohol and acetone and embedded in Epon 812 overnight. Next, ultra-thin 60-80 nm sections were

cut with a diamond knife using a Leica Ultracut UCT (Leica Microsystems GmbH, Wetzlar, Germany) and stained with uranyl acetate and lead citrate. The ultrastructures of the tight junctions were observed using a HITACHI U8010 transmission electron microscope (Hitachi, Ltd., Tokyo, Japan).

**Isolation of CD11c<sup>+</sup> LPMPs.** At 8 weeks after *Trichinella spiralis* infection, CD11c<sup>+</sup> LPMPs were isolated from the intestines of the PI-IBS and normal mice. The entire small intestine was collected from each mouse, cut open longitudinally, washed with PBS, and then cut into 0.5-cm pieces. Subsequently, the tissue pieces were incubated in PBS supplemented with 5% fetal bovine serum (FBS) (Life Technologies, Gaithersburg, MD, USA), EDTA (1 mM), DTT (1 mM), and penicillin (100 Units/ml)/streptomycin (100 µg/ml) (1%; Life Technologies) at 37°C for 20 min, followed by removal of the epithelium. This incubation/epithelial removal step was repeated twice, and then the tissues were cut into smaller pieces and subsequently digested with 1 mg/ml collagenase IV (Roche Diagnostics, Basel, Switzerland) in RPMI-1640 medium (Life Technologies) at 37°C for 60 min. Next, the cell suspension was sequentially filtered through 100-µm and 400-µm filters and washed with RPMI-1640. LPMCs were harvested using a discontinuous 40%/75% Percoll gradient (GE Healthcare, Chalfont, UK). After being washed and resuspended in MACS buffer, the LPMCs were incubated with a microbead-conjugated anti-CD11c antibody (Miltenyi Biotec GmbH, Bergisch Gladbach, Germany). CD11c<sup>+</sup> LPMPs were selected using MACS columns (Miltenyi Biotec GmbH). The selected cells were routinely found to contain ~85% CD11c<sup>+</sup> cells based on flow cytometry. Cell viability did not fall below 90% based on trypan blue exclusion assays.

**Adoptive transfer of CD11c<sup>+</sup> LPMPs.** CD11c<sup>+</sup> LPMPs were generated in mice with or without *Trichinella* infection and were then adoptively transferred into NIH Swiss mice. Each mouse was administered 1×10<sup>6</sup> CD11c<sup>+</sup> LPMPs via intravenous injection into the tail. At 120 h after the transfer of CD11c<sup>+</sup> LPMPs, AWR scores were determined. Intestinal tissues were collected for permeability assays and analysis of intestinal inflammation. More than six mice were included in each group.

**Western blot analysis.** Intestinal tissues were homogenized via mechanical disruption in RIPA buffer with a protease inhibitor cocktail (EDTA-free; Roche Diagnostics). The samples were then clarified via centrifugation at 12,000 rpm for 10 min at 4°C. Next, the supernatants were diluted with loading buffer and heated to 95°C for 10 min. Subsequently, protein concentrations were determined using a BCA protein assay kit (Thermo Fisher Scientific, Waltham, MA, USA). The samples were separated on 10-12% SDS-PAGE gels and transferred to polyvinylidene fluoride membranes (Millipore, Billerica, MA, USA). The membranes were then probed overnight at 4°C with antibodies against the TNF-α (goat anti-mouse; AF-410-NA), IL-4 (rat anti-mouse; MAB404) and IL-10 (rat anti-mouse; MAB417) cytokines (1 µg/ml, all from R&D Systems, Minneapolis, MN, USA), occludin-1 (rabbit anti-mouse; 71-1500) and claudin-1 (rabbit anti-mouse; 51-9000) (1.25 µg/ml; both from Life Technologies) or Gapdh (rabbit anti-mouse; ABS16; 0.5 µg/ml; Millipore)

and were then probed with HRP-conjugated secondary antibodies [goat anti-rabbit IgG (111-035-003), goat anti-rat IgG (112-035-003) and rabbit anti-goat IgG (305-035-003); 0.25 µg/ml; Jackson ImmunoResearch Laboratories, Inc., West Grove, PA, USA] at room temperature for 2 h. The results were analyzed with Quantity One 4.6.2 software (Bio-Rad Laboratories, Inc., Hercules, CA, USA). More than six mice were included in each group.

**Data analysis.** The AWR scores were compared using the Kruskal-Wallis one-way analysis of variance (ANOVA) on ranks test, and significant results ( $P < 0.05$ ) were further analyzed using the Wilcoxon rank sum test with Bonferroni correction for multiple comparisons (0.05/3). The other data are expressed as the mean ± SE and were analyzed via one-way ANOVA, followed by the least significant difference (LSD) test or Dunnett's T3 multiple range test.  $P < 0.05$  was considered to indicate a statistically significant difference. Statistical analyses were performed with SPSS version 19.0 (IBM SPSS, Armonk, NY, USA).

## Results

**Assessment of intestinal inflammation after *Trichinella* infection.** Severe inflammation was observed at 2 weeks post-infection; however, no discernible inflammation was detected at 8 weeks post-infection (Fig. 1A). H&E staining revealed that hyperemia, swelling and severe neutrophilic and eosinophilic infiltration were induced in the whole gut by *Trichinella* at 2 weeks post-infection. However, no obvious microscopic changes were observed at 8 weeks post-infection.

Next, we examined the cytokine expression levels to determine whether a T helper 1 or T helper 2 immune response was involved in the intestinal inflammatory response. IL-4 expression in the ileum was found to be significantly elevated at 8 weeks post-infection compared with that in the control mice and mice at 2 weeks post-infection ( $p = 0.046$ ;  $p = 0.001$ ); however, no significant difference in IL-10 or TNF-α expression was observed among these groups of mice (Fig. 1B). These results suggested that *Trichinella* infection in the chronic stage might be associated with a T helper 2 response.

**AWR scores after infection.** The AWR scores began to increase during the 2nd week post-infection, and they remained elevated during the 8th week at CRD intensities of 40 and 60 mmHg (Fig. 2A). Similarly, the thresholds of the 2- and 8-week post-infection groups were lower than those of the control group (Fig. 2B). These results implied that visceral hyperalgesia was sustained even though intestinal inflammation had subsided by the 8th week after infection, and they further suggested that the 8-week post-infection group was a better model for PI-IBS with visceral hypersensitivity.

**Increased mucosal permeability after infection.** Next, we used a Ussing chamber system to examine transepithelial electrical resistance and FD4 flux to evaluate intestinal epithelial barrier function in the ileum after infection (Fig. 3).

The transepithelial electrical resistance of the ileal villus epithelium was decreased in both the 2- and 8-week post-infection groups compared with the control group ( $42.60 \pm 2.51$  vs.  $53.87 \pm 3.55$ ,  $P = 0.008$ ;  $40.61 \pm 1.95$  vs.  $3.87 \pm 3.55$ ,

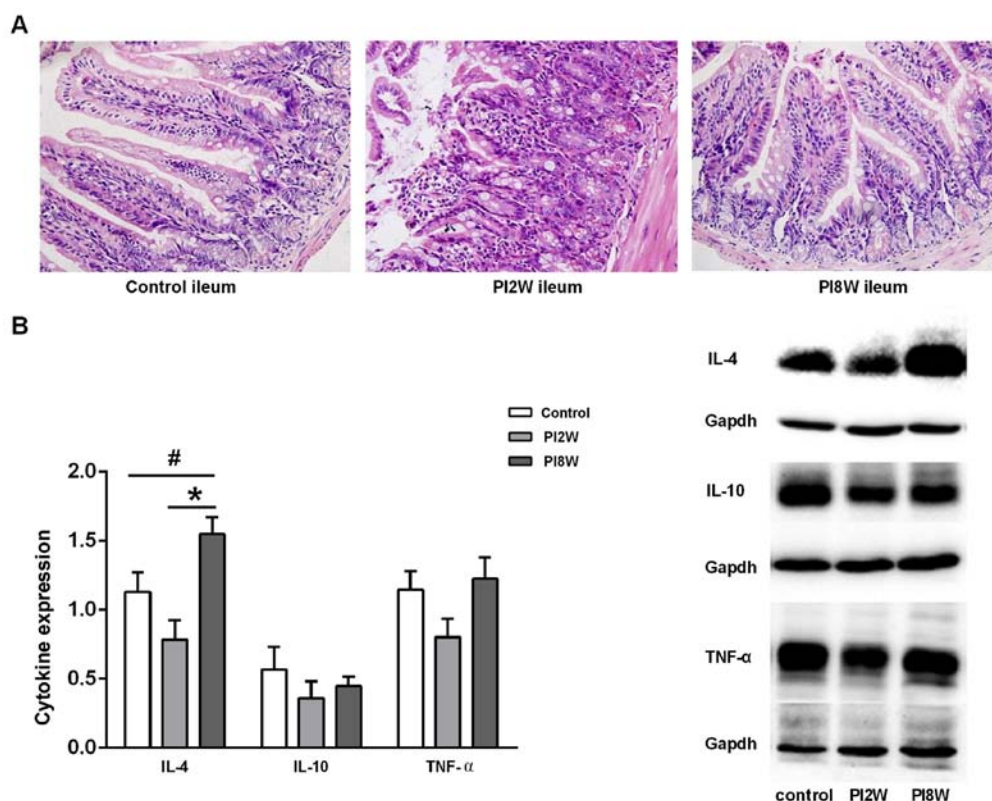


Figure 1. Assessment of intestinal inflammation after *Trichinella* infection. (A) Representative H&E-stained paraffin sections of ilea from mice in the control and PI2W and PI8W groups; magnification, x400. (B) Cytokine expression in the ileum. The data are presented as the mean  $\pm$  SE;  $n \geq 6$  mice per group. <sup>#</sup> $P < 0.05$  for the PI2W and PI8W groups vs. the control group; <sup>\*</sup> $P < 0.05$  for the PI2W group vs. the PI8W group. H&E, hematoxylin and eosin; SE, standard error; PI2W, 2 weeks post-infection; PI8W, 8 weeks post-infection.

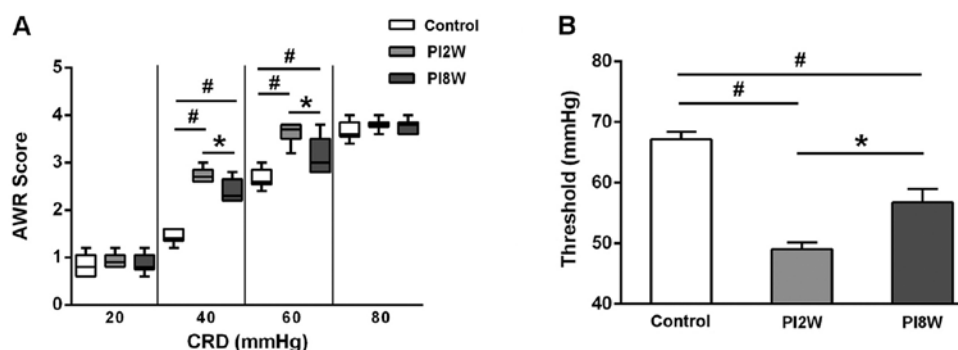


Figure 2. Changes in visceral sensation after infection. The AWR scores and thresholds recorded in the response to CRD for the three groups. (A) Box plot of the AWR scores. The lines in the boxes represent the medians, and the lines at the ends of the boxes represent the 25th and 75th percentiles. The error bars denote the 5th and 95th percentiles;  $n \geq 6$  mice per group. (B) The threshold CRD intensities that evoked abdominal contractions in the mice are displayed as the mean  $\pm$  SE;  $n \geq 6$  mice per group. <sup>#</sup> $P < 0.05$  for the PI2W and PI8W groups vs. the control group; <sup>\*</sup> $P < 0.05$  for the PI2W group vs. the PI8W group. AWR, abdominal withdrawal reflex; CRD, colorectal distention; SE, standard error; PI2W, 2 weeks post-infection; PI8W, 8 weeks post-infection.

$P = 0.002$ ) (Fig. 3A). In contrast, FD4 flux, which reflects the barrier function of the paracellular pathways, exhibited a drastic increase in the ileal villus epithelium ( $P = 0.001$ ) (Fig. 3B). These results suggested that intestinal permeability increased immediately post-infection and that it remained elevated, even at 8 weeks when intestinal inflammation had subsided. To further identify which paracellular pathway was affected, we focused on the tight junctions and analyzed the occludin-1 and claudin-1 expression levels. As shown in Fig. 3C, occludin-1 and claudin-1 expression in the ileum were downregulated in the 2-week post-infection group compared with the control

group ( $p = 0.034$ ;  $p = 0.021$ ); further, their expression was slightly but non-significantly downregulated in the 8-week group compared with the control group (Fig. 3C).

**Milder inflammation after adoptive transfer of CD11c<sup>+</sup> LPMPs from PI-IBS mice.** CD11c<sup>+</sup> LPMPs were isolated from the intestines of PI-IBS mice and normal mice at 8 weeks after *T. spiralis* infection. The mice that received CD11c<sup>+</sup> LPMPs from the PI-IBS or normal mice displayed inconspicuous microscopic inflammation, as visualized by H&E staining (Fig. 4A). No significant differences in the

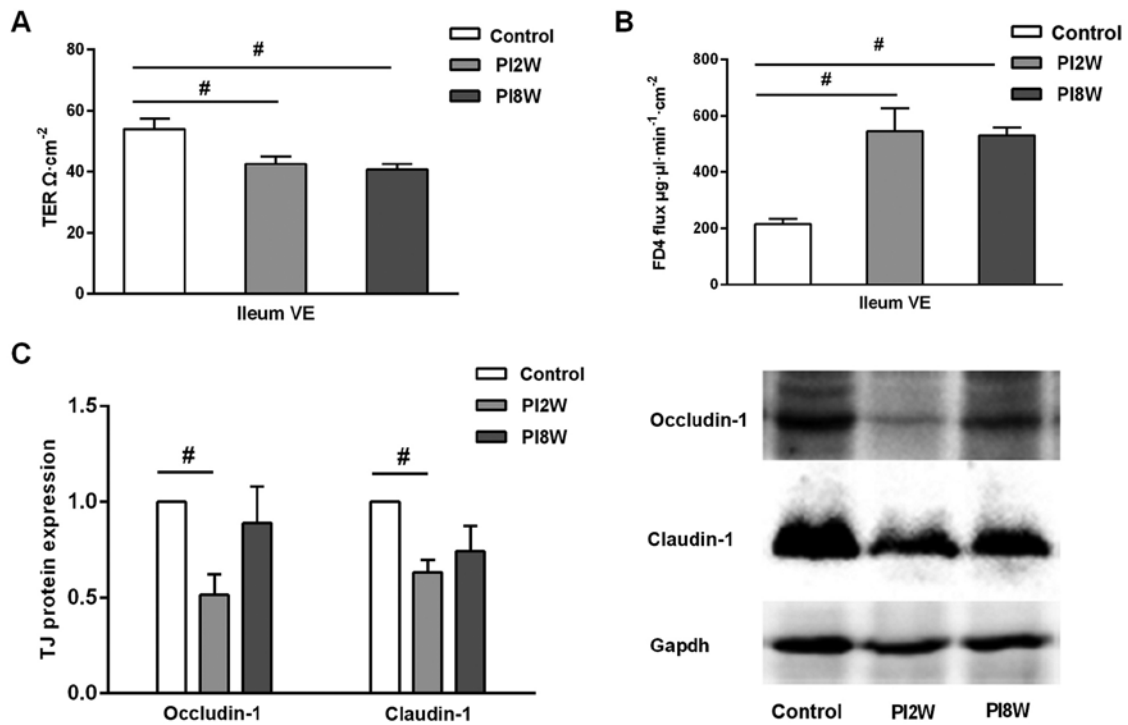


Figure 3. Mucosal permeability is increased after infection. (A) TER of the ileal VE in the control, PI2W and PI8W groups. (B) FD4 fluxes in the three groups. (C) Expression of the tight junction (TJ) proteins occludin-1 and claudin-1 in the ileum. All data are presented as the mean  $\pm$  SE;  $n \geq 6$  mice per group.  $^{\#}P < 0.05$  for the PI2W and PI8W groups vs. the control group. PI2W, 2 weeks post-infection; PI8W, 8 weeks post-infection. TER, transepithelial electrical resistance; VE, villus epithelium; SE, standard error.

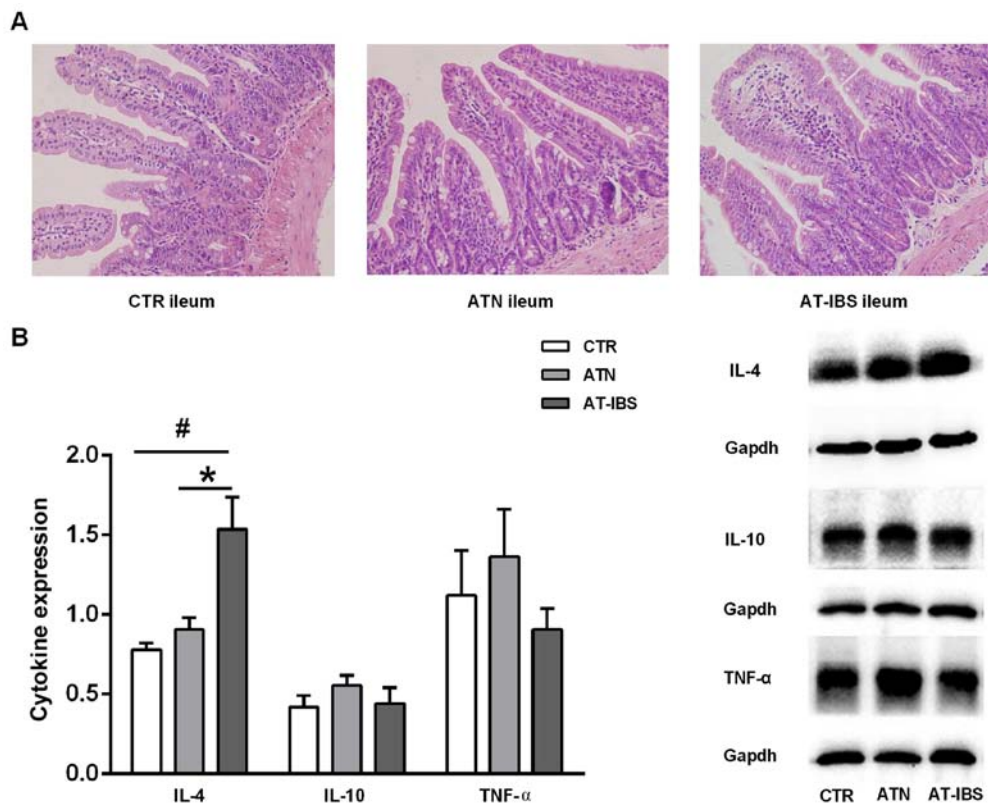


Figure 4. Milder inflammation after the adoptive transfer of CD11c<sup>+</sup> LPMPs from PI-IBS mice into naïve mice. (A) Representative H&E-stained sections of ilea from the CTR, ATN and AT-IBS groups; magnification,  $\times 400$ . (B) Cytokine profiles in the ileum. The data are presented as the mean  $\pm$  SE;  $n \geq 6$  mice per group. ATN, adoptive transfer of CD11c<sup>+</sup> LPMPs from normal mice; AT-IBS, adoptive transfer of CD11c<sup>+</sup> LPMPs from PI-IBS mice; CTR, control mice injected with the same volume of saline.  $^{\#}P < 0.05$  for the ATN and AT-IBS groups vs. the CTR group;  $^*P < 0.05$  for the ATN group vs. the AT-IBS group. The ATN group was included in this study to ensure that CD11c<sup>+</sup> LPMPs were the only variable in the experiment and to eliminate effects of the adoptive transfer on the experimental results. LPMPs, lamina propria mononuclear phagocytes; PI-IBS, post-infectious irritable bowel syndrome; H&E, hematoxylin and eosin.

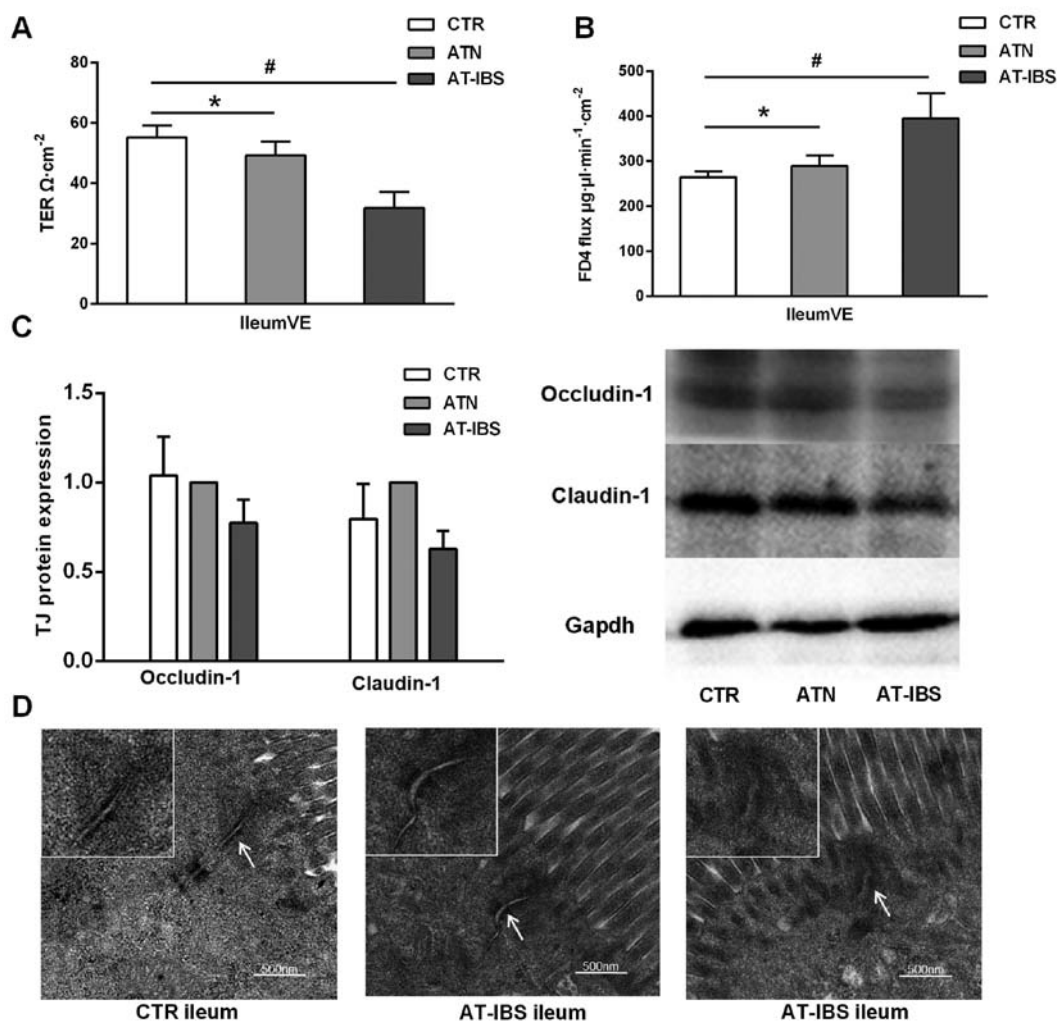


Figure 5. Increased intestinal permeability after adoptive transfer of CD11c<sup>+</sup> LPMPs from PI-IBS mice. (A) TER of the ileal VE in the CTR, ATN and AT-IBS groups. (B) FD4 fluxes in the three groups. (C) Expression of the tight junction (TJ) proteins occludin-1 and claudin-1 in the ileum. All data are presented as the mean  $\pm$  SE;  $n \geq 6$  mice per group. (D) Tight junction ultrastructure, as determined by transmission electron microscopy. The arrows indicate tight junctions. The mice in the AT-IBS group exhibited increases in the apical intercellular distance and proportion of dilated junctions, as well as perijunctional cytoskeletal condensation. ATN, adoptive transfer of CD11c<sup>+</sup> LPMPs from normal mice; AT-IBS, adoptive transfer of CD11c<sup>+</sup> LPMPs from PI-IBS mice; CTR, control mice injected with the same volume of saline.  $^{\#}P < 0.05$  for the ATN and AT-IBS groups vs. the CTR group;  $^{*}P < 0.05$  for the ATN group vs. the AT-IBS group. The ATN group was included in this study to ensure that CD11c<sup>+</sup> LPMPs were the only variables in the experiment and to eliminate effects of the adoptive transfer on the experimental results. LPMPs, lamina propria mononuclear phagocytes; PI-IBS, post-infectious irritable bowel syndrome; TER, transepithelial electrical resistance; VE, villus epithelium; SE, standard error.

histological characteristics were observed between the mice that received CD11c<sup>+</sup> LPMPs from the PI-IBS mice (AT-IBS group), those that received CD11c<sup>+</sup> LPMPs from the normal mice (ATN group), and the untreated mice (CTR group). The ATN group was included in this study to ensure that CD11c<sup>+</sup> LPMPs were the only variable in the experiment and to eliminate effects of the adoptive transfer on the experimental results. Although no inflammation or damage was observed in the microscopic examinations, increased IL-4 expression was detected in the ilea of the AT-IBS mice compared with that in the ilea of the CTR and ATN mice ( $P = 0.019$ ;  $P = 0.048$ ). There was no difference in IL-10 or TNF- $\alpha$  expression in the ileum between the CTR, ATN and AT-IBS mice (Fig. 4B).

**Increased intestinal permeability after adoptive transfer of CD11c<sup>+</sup> LPMPs from PI-IBS mice.** The transfer of CD11c<sup>+</sup> LPMPs from PI-IBS mice resulted in decreased transepithelial

electrical resistance in the ileal villus epithelium compared with that in the CTR and ATN mice ( $31.68 \pm 5.41$  vs.  $55.23 \pm 3.81$ ,  $P = 0.001$ ;  $31.68 \pm 5.41$  vs.  $49.23 \pm 4.54$ ,  $P = 0.008$ ) (Fig. 5A). In contrast, the FD4 flux in the ileal villus epithelium was increased following CD11c<sup>+</sup> LPMP transfer ( $P = 0.043$ ) (Fig. 5B). These results suggested that intestinal permeability was increased in the ileal villus epithelium. Furthermore, tight junction protein expression was slightly but non-significantly downregulated in the AT-IBS mice compared with that in the CTR and ATN mice (Fig. 5C).

However, ultrastructural alterations of tight junction proteins were detected in the mice that received CD11c<sup>+</sup> LPMPs from the PI-IBS mice. As previously described, the routine H&E staining performed in the present study revealed no differences in epithelial architecture between the control and adoptive transfer groups. Transmission electron microscopy imaging showed that the functional alterations described



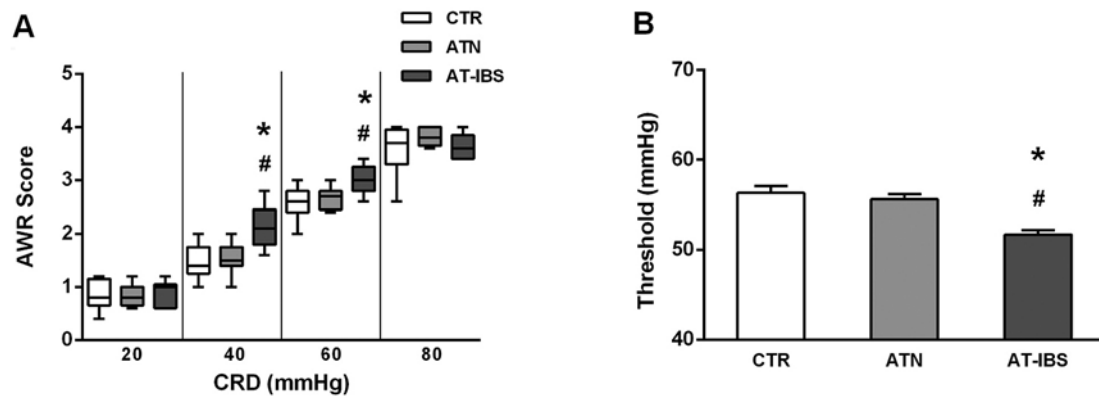


Figure 6. Changes in visceral sensation after adoptive transfer of CD11c<sup>+</sup> LPMPs. (A) Box plot of the AWR scores obtained at 20, 40, 60 and 80 mmHg. The lines in the boxes represent the medians, and the lines at the ends of the boxes represent the 25th and 75th percentiles. The error bars denote the 5th and 95th percentiles;  $n \geq 6$  mice per group. (B) Thresholds at various CRD intensities. The means  $\pm$  SEs are plotted;  $n \geq 6$  mice per group. ATN, adoptive transfer of CD11c<sup>+</sup> LPMPs from normal mice; AT-IBS, adoptive transfer of CD11c<sup>+</sup> LPMPs from PI-IBS mice; CTR, control mice injected with the same volume of saline. \* $P < 0.05$  for the ATN and AT-IBS groups vs. the CTR group; # $P < 0.05$  for the ATN group vs. the AT-IBS group. The ATN group was included in this study to ensure that CD11c<sup>+</sup> LPMPs were the only variable in the experiment and to eliminate effects of the adoptive transfer on the experimental results. LPMPs, lamina propria mononuclear phagocytes; AWR, abdominal withdrawal reflex; CRD, colorectal distension; SE, standard error; PI-IBS, post-infectious irritable bowel syndrome.

above were associated with ultrastructural changes in the intercellular junctions, including disassembly (Fig. 5D). The mice that received CD11c<sup>+</sup> LPMPs from the PI-IBS mice exhibited increases in the apical intercellular distance and proportion of dilated junctions compared with the controls. These mice also displayed a greater number of junctions with perijunctional cytoskeletal condensation (Fig. 5D).

**Changes in visceral sensation after adoptive transfer of CD11c<sup>+</sup> LPMPs.** Finally, we examined visceral sensation after CD11c<sup>+</sup> LPMP transfer. As illustrated in Fig. 6, the mice that received CD11c<sup>+</sup> LPMPs from PI-IBS mice exhibited greater visceral sensitivity. Significant increases in the AWR scores were observed at pressures of 40 and 60 mmHg compared with those of the control mice (Fig. 6A). Similarly, the thresholds were lower following the adoptive transfer of CD11c<sup>+</sup> LPMPs from the PI-IBS mice (Fig. 6B); consequently, the mice that received these cells exhibited visceral hypersensitivity.

## Discussion

In the present study, we demonstrated that increased intestinal permeability, visceral hypersensitivity and intestinal inflammation were present during both the acute and chronic stages of *Trichinella* infection. Even after expulsion of the parasite, these changes persisted in the PI-IBS stage. The transfer of CD11c<sup>+</sup> LPMPs from PI-IBS mice into naïve mice not only resulted in the transfer of enteric inflammation but also caused abnormal intestinal function, characterized by epithelial barrier disruption and visceral hyperalgesia.

To better understand the role of CD11c<sup>+</sup> LPMPs in sustained inflammation associated with PI-IBS, we employed a direct method of adoptive transfer. As previously described, CD11c<sup>+</sup> LPMPs in PI-IBS mice secrete several cytokines to induce T-cell differentiation into the Th1, Th2 and Th17 subtypes (29). Therefore, to identify the immune responses induced by CD11c<sup>+</sup> LPMPs, these cells were adoptively transferred from

PI-IBS mice into naïve mice. Although microscopic examinations did not reveal any obvious inflammation following adoptive transfer, mild inflammation was noted based on the cytokine profiles in the small intestine. An increase in IL-4 expression, implicating the T helper 2 response, was detected in the ilea of the mice that received CD11c<sup>+</sup> LPMPs from the PI-IBS mice compared with that in the ilea of the controls. Previous studies have shown that certain subtypes of mononuclear phagocytes can be transferred to inflammatory bowel disease model mice to promote or relieve colitis (37-39); however, the adoptive transfer of CD11c<sup>+</sup> LPMPs from PI-IBS mice has not been previously reported. Thus, our study is the first to report that the relatively mild inflammation in PI-IBS mice can be transferred to naïve mice via CD11c<sup>+</sup> LPMPs.

More importantly, the increased permeability and inflammation observed in the PI-IBS mouse model could also be transferred by CD11c<sup>+</sup> LPMPs. The mice that received CD11c<sup>+</sup> LPMPs from PI-IBS mice exhibited decreased transepithelial electrical resistance and increased FD4 fluorescence intensity in the ileal villus epithelium. Although no significant changes in the expression of tight junction proteins were observed, ultrastructural alterations of tight junctions were detected in the ileum by transmission electron microscopy. Previous studies have shown that a number of cytokines, including IL-4, TNF- $\alpha$  and IL-6, cause changes in tight junction permeability (35,40-44). Therefore, the low-grade inflammation marked by increased IL-4 expression observed in our study may have contributed to the barrier dysfunction in the PI-IBS mice.

All of these findings indicate that mild inflammation caused by the adoptive transfer of CD11c<sup>+</sup> LPMPs results in increased epithelial permeability. The decreased transepithelial electrical resistance and increased FD4 fluorescence intensity in the ileal villus epithelium observed in the PI-IBS and AT-IBS mice are suggestive of increased permeability of the intestinal epithelial cell barrier that is dependent on the villus epithelial pathway.

In addition to barrier dysfunction, the visceral hypersensitivity of the PI-IBS mice was also found to be transferred by CD11c<sup>+</sup> LPMPs. Significant increases in the AWR scores were observed at intensities of 40 and 60 mmHg, and the thresholds decreased following the adoptive transfer of CD11c<sup>+</sup> LPMPs from the PI-IBS mice. The changes in visceral sensation observed in the present study may have resulted from a combined process of barrier dysfunction and mild mucosal inflammation induced by CD11c<sup>+</sup> LPMP transfer. Our results showed that the increases in visceral sensitivity, intestinal permeability and IL-4 expression, as well as the histological characteristics, were consistent in both the PI-IBS and AT-IBS animal model groups. Therefore, our findings strongly imply that CD11c<sup>+</sup> LPMPs play an important role in the development of PI-IBS.

In the present study, in addition to obvious visceral hypersensitivity and increased mucosal permeability, severe inflammation was detected in the intestinal mucosa during the acute infection stage. After expulsion of the parasites, persistent low-grade inflammation was present, as indicated by the increased cytokine levels. Furthermore, visceral hyperalgesia and barrier dysfunction were sustained. The major characteristics of IBS include visceral hypersensitivity, altered secretion, intestinal sensory nerve abnormalities, barrier dysfunction and alterations in intestinal immune function. Consequently, mouse models of PI-IBS based on *T. spiralis* infection are widely used to investigate both the immunological and functional changes associated with gut inflammation, as described in previous studies (45,46).

In conclusion, we demonstrated that increased mucosal permeability and visceral hypersensitivity were maintained, even under conditions of mild inflammation, in the studied PI-IBS mouse model. CD11c<sup>+</sup> LPMPs from these mice were able to transfer not only enteric inflammation but also abnormal intestinal function, characterized by epithelial barrier disruption and visceral hyperalgesia, to normal mice. These findings may contribute to the current understanding of the role of mild inflammation in the pathophysiology of PI-IBS.

## Acknowledgements

The present study was supported by the National Natural Science Foundation of China (grant nos. 81500415 and 81330014). The website is <http://www.nsfc.gov.cn/>.

## References

- Shen L and Turner JR: Role of epithelial cells in initiation and propagation of intestinal inflammation. Eliminating the static: Tight junction dynamics exposed. *Am J Physiol Gastrointest Liver Physiol* 290: G577-G582, 2006.
- Turner JR: Intestinal mucosal barrier function in health and disease. *Nat Rev Immunol* 9: 799-809, 2009.
- Martínez C, Lobo B, Pigrau M, Ramos L, González-Castro AM, Alonso C, Guilarte M, Guilá M, de Torres I, Azpiroz F, *et al*: Diarrhoea-predominant irritable bowel syndrome: An organic disorder with structural abnormalities in the jejunal epithelial barrier. *Gut* 62: 1160-1168, 2013.
- Keszthelyi D, Troost FJ, Jonkers DM, van Eijk HM, Lindsey PJ, Dekker J, Buurman WA and Masclee AA: Serotonergic reinforcement of intestinal barrier function is impaired in irritable bowel syndrome. *Aliment Pharmacol Ther* 40: 392-402, 2014.
- Cheng P, Yao J, Wang C, Zhang L and Kong W: Molecular and cellular mechanisms of tight junction dysfunction in the irritable bowel syndrome. *Mol Med Rep* 12: 3257-3264, 2015.
- Barbara G: Mucosal barrier defects in irritable bowel syndrome. Who left the door open? *Am J Gastroenterol* 101: 1295-1298, 2006.
- Camilleri M and Gorman H: Intestinal permeability and irritable bowel syndrome. *Neurogastroenterol Motil* 19: 545-552, 2007.
- Dunlop SP, Hebden J, Campbell E, Naesdal J, Olbe L, Perkins AC and Spiller RC: Abnormal intestinal permeability in subgroups of diarrhea-predominant irritable bowel syndromes. *Am J Gastroenterol* 101: 1288-1294, 2006.
- Piche T, Barbara G, Aubert P, Bruley des Varannes S, Dainese R, Nano JL, Cremon C, Stanghellini V, De Giorgio R, Galmiche JP, *et al*: Impaired intestinal barrier integrity in the colon of patients with irritable bowel syndrome: Involvement of soluble mediators. *Gut* 58: 196-201, 2009.
- Thabane M and Marshall JK: Post-infectious irritable bowel syndrome. *World J Gastroenterol* 15: 3591-3596, 2009.
- Spiller RC, Jenkins D, Thornley JP, Hebden JM, Wright T, Skinner M and Neal KR: Increased rectal mucosal enteroendocrine cells, T lymphocytes, and increased gut permeability following acute *Campylobacter* enteritis and in post-dysenteric irritable bowel syndrome. *Gut* 47: 804-811, 2000.
- Guilarte M, Santos J, de Torres I, Alonso C, Vicario M, Ramos L, Martínez C, Casellas F, Saperas E and Malagelada JR: Diarrhoea-predominant IBS patients show mast cell activation and hyperplasia in the jejunum. *Gut* 56: 203-209, 2007.
- Walker MM, Talley NJ, Prabhakar M, Pennaneach CJ, Aro P, Ronkainen J, Storskrubb T, Harmsen WS, Zinsmeister AR and Agreus L: Duodenal mastocytosis, eosinophilia and intraepithelial lymphocytosis as possible disease markers in the irritable bowel syndrome and functional dyspepsia. *Aliment Pharmacol Ther* 29: 765-773, 2009.
- Ohman L and Simrén M: Pathogenesis of IBS: Role of inflammation, immunity and neuroimmune interactions. *Nat Rev Gastroenterol Hepatol* 7: 163-173, 2010.
- Sundin J, Rangel I, Kumawat AK, Hultgren-Hörnquist E and Brummer RJ: Aberrant mucosal lymphocyte number and subsets in the colon of post-infectious irritable bowel syndrome patients. *Scand J Gastroenterol* 49: 1068-1075, 2014.
- Bhuiyan MR, Majumder TK, Raihan AA, Roy PK, Farha N and Kamal M: Histopathological alterations in post-infectious irritable bowel syndrome in Bangladeshi population. *Mymensingh Med J* 19: 275-281, 2010.
- Kirsch R and Riddell RH: Histopathological alterations in irritable bowel syndrome. *Mod Pathol* 19: 1638-1645, 2006.
- Gwee KA, Collins SM, Read NW, Rajnakova A, Deng Y, Graham JC, McKendrick MW and Mouchhala SM: Increased rectal mucosal expression of interleukin 1beta in recently acquired post-infectious irritable bowel syndrome. *Gut* 52: 523-526, 2003.
- Chen J, Zhang Y and Deng Z: Imbalanced shift of cytokine expression between T helper 1 and T helper 2 (Th1/Th2) in intestinal mucosa of patients with post-infectious irritable bowel syndrome. *BMC Gastroenterol* 12: 91, 2012.
- Feng B, La JH, Schwartz ES and Gebhart GF: Irritable bowel syndrome: Methods, mechanisms, and pathophysiology. Neural and neuro-immune mechanisms of visceral hypersensitivity in irritable bowel syndrome. *Am J Physiol Gastrointest Liver Physiol* 302: G1085-G1098, 2012.
- Scott CL, Henri S and Williams M: Mononuclear phagocytes of the intestine, the skin, and the lung. *Immunol Rev* 262: 9-24, 2014.
- Huang H, Liu JQ, Yu Y, Mo LH, Ge RT, Zhang HP, Liu ZG, Zheng PY and Yang PC: Regulation of TWIK-related potassium channel-1 (Trek1) restitutes intestinal epithelial barrier function. *Cell Mol Immunol* 13: 110-118, 2016.
- Arnold IC, Mathisen S, Schulthess J, Danne C, Hegazy AN and Powrie F: CD11c(+) monocyte/macrophages promote chronic *Helicobacter hepaticus*-induced intestinal inflammation through the production of IL-23. *Mucosal Immunol* 9: 352-363, 2016.
- Aycheh T, Mildner A, Yona S, Kim KW, Lampl N, Reich-Zeliger S, Boon L, Yorgev N, Waisman A, Cua DJ, *et al*: IL-23-mediated mononuclear phagocyte crosstalk protects mice from *Citrobacter rodentium*-induced colon immunopathology. *Nat Commun* 6: 6525, 2015.
- Hart AL, Al-Hassi HO, Rigby RJ, Bell SJ, Emmanuel AV, Knight SC, Kamm MA and Stagg AJ: Characteristics of intestinal dendritic cells in inflammatory bowel diseases. *Gastroenterology* 129: 50-65, 2005.
- Silva MA, López CB, Riverin F, Oligny L, Menezes J and Seidman EG: Characterization and distribution of colonic dendritic cells in Crohn's disease. *Inflamm Bowel Dis* 10: 504-512, 2004.



27. Krajina T, Leithäuser F, Möller P, Trobonjaca Z and Reimann J: Colonic lamina propria dendritic cells in mice with CD4<sup>+</sup> T cell-induced colitis. *Eur J Immunol* 33: 1073-1083, 2003.
28. Karlis J, Penttilä I, Tran TB, Jones B, Nobbs S, Zola H and Flesch IE: Characterization of colonic and mesenteric lymph node dendritic cell subpopulations in a murine adoptive transfer model of inflammatory bowel disease. *Inflamm Bowel Dis* 10: 834-847, 2004.
29. Long Y, Wang W, Wang H, Hao L, Qian W and Hou X: Characteristics of intestinal lamina propria dendritic cells in a mouse model of postinfectious irritable bowel syndrome. *J Gastroenterol Hepatol* 27: 935-944, 2012.
30. Li M, Zhang L, Lu B, Chen Z, Chu L, Meng L and Fan Y: Role of dendritic cell-mediated abnormal immune response in visceral hypersensitivity. *Int J Clin Exp Med* 8: 13243-13250, 2015.
31. Jones RC III, Otsuka E, Wagstrom E, Jensen CS, Price MP and Gebhart GF: Short-term sensitization of colon mechanoreceptors is associated with long-term hypersensitivity to colon distention in the mouse. *Gastroenterology* 133: 184-194, 2007.
32. Al-Chaer ED, Kawasaki M and Pasricha PJ: A new model of chronic visceral hypersensitivity in adult rats induced by colon irritation during postnatal development. *Gastroenterology* 119: 1276-1285, 2000.
33. Velin AK, Ericson AC, Braaf Y, Wallon C and Söderholm JD: Increased antigen and bacterial uptake in follicle associated epithelium induced by chronic psychological stress in rats. *Gut* 53: 494-500, 2004.
34. Keita AV, Söderholm JD and Ericson AC: Stress-induced barrier disruption of rat follicle-associated epithelium involves corticotropin-releasing hormone, acetylcholine, substance P, and mast cells. *Neurogastroenterol Motil* 22: 770-778, 2010.
35. Overman EL, Rivier JE and Moeser AJ: CRF induces intestinal epithelial barrier injury via the release of mast cell proteases and TNF- $\alpha$ . *PLoS One* 7: e39935, 2012.
36. Pozzo Miller LD and Landis DM: Cytoplasmic structure in organotypic cultures of rat hippocampus prepared by rapid freezing and freeze-substitution fixation. *Synapse* 13: 195-205, 1993.
37. Siddiqui KR, Laffont S and Powrie F: E-cadherin marks a subset of inflammatory dendritic cells that promote T cell-mediated colitis. *Immunity* 32: 557-567, 2010.
38. McDole JR, Wheeler LW, McDonald KG, Wang B, Konjufca V, Knoop KA, Newberry RD and Miller MJ: Goblet cells deliver luminal antigen to CD103<sup>+</sup> dendritic cells in the small intestine. *Nature* 483: 345-349, 2012.
39. Cascio JA, Haymaker CL, Divekar RD, Zaghoulani S, Khairallah MT, Wan X, Rowland LM, Dhakal M, Chen W and Zaghoulani H: Antigen-specific effector CD4 T lymphocytes school lamina propria dendritic cells to transfer innate tolerance. *J Immunol* 190: 6004-6014, 2013.
40. Poritz LS, Garver KI, Tilberg AF and Koltun WA: Tumor necrosis factor alpha disrupts tight junction assembly. *J Surg Res* 116: 14-18, 2004.
41. McDermott JR, Bartram RE, Knight PA, Miller HR, Garrod DR and Grecis RK: Mast cells disrupt epithelial barrier function during enteric nematode infection. *Proc Natl Acad Sci USA* 100: 7761-7766, 2003.
42. Edelblum KL and Turner JR: The tight junction in inflammatory disease: Communication breakdown. *Curr Opin Pharmacol* 9: 715-720, 2009.
43. Al-Sadi R, Ye D, Boivin M, Guo S, Hashimi M, Ereifej L and Ma TY: Interleukin-6 modulation of intestinal epithelial tight junction permeability is mediated by JNK pathway activation of claudin-2 gene. *PLoS One* 9: e85345, 2014.
44. Al-Sadi R, Boivin M and Ma T: Mechanism of cytokine modulation of epithelial tight junction barrier. *Front Biosci (Landmark Ed)* 14: 2765-2778, 2009.
45. Bercík P, Wang L, Verdú EF, Mao YK, Blennerhassett P, Khan WI, Kean I, Tougas G and Collins SM: Visceral hyperalgesia and intestinal dysmotility in a mouse model of postinfective gut dysfunction. *Gastroenterology* 127: 179-187, 2004.
46. Fu Y, Wang W, Tong J, Pan Q, Long Y, Qian W and Hou X: Th17 cells influence intestinal muscle contraction during *Trichinella spiralis* infection. *J Huazhong Univ Sci Technolog Med Sci* 29: 481-485, 2009.